ANTICANCER RESEARCH *38*: 1511-1516 (2018)
doi:10.21873/anticanres.12378

Dose–function Histogram Evaluation Using ^{99m}Tc-GSA SPECT/CT Images for Stereotactic Body Radiation Therapy Planning for Hepatocellular Carcinoma Patients: A Dosimetric Parameter Comparison

RYO TOYA[1], TETSUO SAITO[1], SHINYA SHIRAISHI[2], YUDAI KAI[3], RYUJI MURAKAMI[4], TOMOHIKO MATSUYAMA[1], TAKAHIRO WATAKABE[1], FUMI SAKAMOTO[2], NORIKO TSUDA[2], YOSHINOBU SHIMOHIGASHI[3], YASUYUKI YAMASHITA[2] and NATSUO OYA[1]

[1]*Department of Radiation Oncology, Kumamoto University Hospital,* [2]*Department of Diagnostic Radiology, Kumamoto University Hospital,* [3]*Department of Radiological Technology, Kumamoto University Hospital,* [4]*Department of Medical Imaging, Faculty of Life Sciences, Kumamoto University, Kumamoto, Japan*

Abstract. *Background/Aim: We evaluated the influence of previous treatments on the parametric discrepancies between dose–volume histograms (DVHs) and dose–function histograms (DFHs) generated based on ^{99m}Tc-GSA SPECT images of hepatocellular carcinoma (HCC) patients treated with stereotactic body radiation therapy (SBRT). Patients and Methods: Twelve patients underwent SBRT at 30-40 Gy. Registration between planning CT and SPECT/CT images was performed, and DFH parameters were calculated as follows: Fx=(sum of the counts within the liver volume receiving a dose of more than x Gy/sum of the counts within the whole liver volume) ×100. The discrepancy between Fx and Vx (Dx) was also calculated. Results: The number of previous treatments for lesions other than SBRT-treated lesions (≥2 vs. <2) exhibited a significant influence on the absolute values of D_{10}, D_{15}, and D_{20} ($p<0.05$). Conclusion: Previous treatment significantly influences the parametric discrepancy between DFH and DVH.*

Primary liver cancer is the third most common cause of cancer death worldwide. Hepatocellular carcinoma (HCC) accounts for 85%-90% of primary liver cancers (1). Stereotactic body radiation therapy (SBRT) for HCC has been introduced as an alternative to standard treatments such as surgical resection and radiofrequency ablation (RFA) (1). SBRT delivers a highly conformal, potent dose of radiation to the tumor in some fractions, while minimizing radiation damage to organs at risk. SBRT provides excellent local control for HCC with a reported control rate of 80-90% (2-4).

HCC response to radiation therapy (RT) exhibits a dose–response relationship (5), but a fine balance is required between delivering a sufficient RT dose to control the HCC and avoiding radiation-induced liver toxicity. Radiation-induced liver injury (RILD), which occurs in 10-20% of HCC patients undergoing SBRT, remains a problematic adverse effect, because of pre-existing liver dysfunctions occurring secondary to comorbid conditions such as hepatitis B/C infection and cirrhosis (3, 4). The percentage of normal liver volume receiving a dose over the threshold dose calculated based on a dose–volume histogram (DVH) is commonly used for determining dose constraints and predicting radiation-induced liver toxicity; however, it has limited predictive ability (6, 7).

A drawback of using DVH for SBRT planning in HCC is the lack of functional information because DVHs are generated based on computed tomography (CT) images, which provide only morphological information. A dose–function histogram (DFH) generated based on single photon emission computed tomography (SPECT) images may facilitate the assessment of the functional status of organs at risk. For treatment planning in lung cancers, Marks *et al.* (8) performed DFH calculation using ^{99m}Tc-labeled macro-aggregated albumin and observed decreases in lung perfusion at, adjacent to, and separate from tumor in 94%, 74%, and 42% of patients, respectively. ^{99m}Tc-labeled diethylene triamine pentaacetate-galactosyl human serum albumin

Correspondence to: Ryo Toya, Department of Radiation Oncology, Kumamoto University Hospital, 1-1-1 Honjo, Chuo-ku, Kumamoto 860-8556, Japan. Tel: +81 963735261, Fax: +81 963624330, e-mail: ryo108@kumamoto-u.ac.jp

Key Words: Hepatocellular carcinoma, stereotactic body radiation therapy, dose–function histogram, dose–volume histogram, radiation-induced liver disease.

Table I. *Patient characteristics*.

Patient No.	Age (years)	Gender	Tumor diameter (mm)	Child–Pugh Class	Score	Total dose (Gy)	Previous treatment for other lesions
1	65	M	19	8	B	30	3
2	63	M	16	6	A	40	4
3	76	M	40	5	A	35	0
4	72	M	18	5	A	40	1
5	62	F	25	7	B	30	1
6	69	M	20	5	A	40	0
7	71	F	32	7	B	30	1
8	79	F	45	5	A	35	3
9	75	M	17	7	B	30	0
10	58	M	31	5	A	30	3
11	63	M	29	5	A	40	4
12	73	M	33	6	A	30	1

Previous treatments included radiofrequency ablation, transarterial chemoembolization, and percutaneous ethanol injection therapy.

(^{99m}Tc-GSA) SPECT provides three-dimensional information of regional liver function (9). ^{99m}Tc-GSA SPECT findings suggest that regional function of patients with liver tumors is inhomogeneous due to previous treatments such as RFA and transarterial chemoembolization (TACE) (10), causing discrepancy between DFH and DVH parameters. However, to our knowledge, DFH calculation using fused images from SPECT and planning CT for SBRT for HCC patients has not been reported.

This study evaluated discrepancy between DFH and DVH parameters and influence of previous treatments on parametric discrepancy for HCC patients who underwent SBRT.

Patients and Methods

Patients. This retrospective study based on prospectively acquired data received institutional review board approval. Written informed consent was obtained from all patients. Between August 2013 and February 2017, 12 consecutive HCC patients (nine men and three women; mean age, 68.8 years; range=58-79 years) were included in this study (Table I). Surgery had been performed in three (25%) patients before treatment. Nine (75%) patients had undergone RFA, TACE, and/or percutaneous ethanol injection therapy (PEIT) for HCC in the liver or remnant liver, and no patient received SBRT before treatment. The mean number of previous treatments for lesions other than SBRT-treated lesions was 1.8 (range=0-4 treatments). All patients underwent ^{99m}Tc-GSA SPECT/CT imaging within 1 month before SBRT planning.

SPECT/CT imaging. We used a SPECT/CT system with dual-head detectors and a 16-row multidetector CT scanner (Symbia T16, Siemens Healthcare, Erlangen, Germany). Hepatic SPECT data (60 steps of 15 s/step, 360˚, 128×128 matrix) were obtained using a gamma camera fitted with a low-to-medium energy general-purpose collimator at 20-35 min after the intravenous injection of ^{99m}Tc-GSA (185 MBq). We acquired 64 projections at 6˚ intervals in the continuous mode. To enable SPECT attenuation correction, non-contrast-enhanced helical CT images were obtained. The scanning parameters were as follows: tube voltage, 120 kVp; tube current, 200-275 mA; rotation time, 0.7 sec; beam collimation, 1.25 mm; beam pitch, 0.87; field of view, 36 cm; matrix, 512×512 pixels; slice thickness, 2 mm; and slice interval, 2 mm. After registration between SPECT and CT images, a CT-derived attenuation-coefficient map was created. For SPECT reconstruction, the ordered-subset expectation maximization algorithm (Flash 3D, Siemens Healthcare, Erlangen, Germany) was used (eight iterations; six subsets). Postprocessing was performed with a 7.8-mm Gaussian filter.

Planning simulation CT and treatment planning. The details of the planning simulation CT and treatment planning are described elsewhere (11). Briefly, we used a LightSpeed RT CT scanner (GE Medical Systems, Waukesha, WI, USA). Patients lay supine, and abdominal compression was applied. Immediately after a dynamic contrast-enhanced scan, a non-helical slow-speed scan with a gantry rotation time of 4 s, slice thickness of 2.5 mm, and slice interval of 2.5 mm was performed.

For planning simulation, the images from the dynamic contrast-enhanced scan and slow-speed scan were exported to the Pinnacle^3 treatment planning system (version 9.2; Phillips Radiation Oncology Systems, Fitchburg, WI, USA) and were registered by hardware arrangement. The structures of the target and organs at risk were delineated based on the slow-speed CT images. Treatment planning was performed using 8-9 coplanar and non-coplanar fields with a 6-MV and/or 10-MV photon beam. A total RT dose of 30-40 Gy in five fractions was prescribed at the 70%-80% isodose line of the maximum dose (Table I). The percentage of normal liver volume (liver − gross tumor volume) receiving a dose of more than 20 Gy (V_{20}) did not exceed 20%. SPECT images were not used for treatment planning.

Calculating the parameters of DFH and DVH. Attenuation-corrected SPECT and CT images and planning CT images, including delineated structures and dose distributions, were transferred to Velocity AI (version 3.0.2; Varian Medical Systems,

Table II. *Difference between Fx and Vx (Dx).*

Patient	Parameter										
	D_5	D_{10}	D_{15}	D_{20}	D_{25}	D_{30}	D_{35}	D_{40}	D_{45}	D_{50}	D_{55}
1	4.3	3.1	1.6	0.9	0.6	0.6	0.5	0.5	NA	NA	NA
2	–0.6	–2.5	–3.4	–2.6	–2.0	–1.6	–1.2	–0.9	–0.7	–0.3	0.1
3	–1.7	0.7	0.9	0.4	0.3	0.3	0.4	0.7	0.8	0.0	NA
4	1.9	2.2	1.5	1.1	0.9	0.8	0.7	0.7	0.7	0.6	0.3
5	–0.9	–1.4	–0.6	–0.1	0.4	0.6	1.0	NA	NA	NA	NA
6	–2.1	–2.4	–2.1	–1.9	–1.6	–1.4	–1.1	–0.8	–0.6	–0.2	0.2
7	2.6	2.4	1.8	1.4	1.2	1.3	0.9	NA	NA	NA	NA
8	6.8	6.7	5.3	3.4	1.6	0.6	0.4	0.7	NA	NA	NA
9	–1.3	–1.6	–0.7	–0.2	0.2	0.3	0.4	NA	NA	NA	NA
10	–1.2	–2.6	–2.1	–1.4	–0.9	–0.5	0.1	0.0	NA	NA	NA
11	0.4	1.2	1.9	1.7	1.5	1.5	1.5	1.5	1.5	1.5	1.4
12	–1.3	–1.0	–0.2	0.3	0.4	0.5	0.5	NA	NA	NA	NA
Maximum value	6.8	6.7	5.3	3.4	1.6	1.5	1.5	1.5	1.5	1.5	1.4
Minimum value	–2.1	–2.6	–3.4	–2.6	–2.0	–1.6	–1.2	–0.9	–0.7	–0.3	0.1
Mean of absolute value	2.09	2.32	1.84	1.28	0.97	0.83	0.73	NA	NA	NA	NA

NA: Not applicable.

Palo Alto, CA, USA). After registration between SPECT and CT images by hardware arrangement, we registered SPECT/CT images onto the planning CT images: a rigid image registration followed by a non-rigid deformable registration. During this process, each SPECT voxel was mapped to a new position based on the transformations used in the CT–CT registration, resulting in new SPECT/CT fused images that were deformably registered with the planning CT images (12). Structures of the irradiated volumes of the liver parenchyma were generated at 5-Gy dose increments, based on the dose distribution information.

DFH parameters were calculated as follows:

Fx=(sum of the counts within the liver volume receiving a dose of more than x Gy/sum of the counts within the whole liver volume) ×100.

DVH parameters were calculated as follows:

Vx=(normal liver volume receiving a dose of more than x Gy/whole normal liver volume) ×100 (6).

Statistical analysis. The difference between Fx and Vx (Dx) was calculated by subtracting Vx from Fx (*i.e.*, Fx − Vx) for each parameter. The effect of the number of previous treatments (of RFA, TACE, and PEIT) for lesions other than SBRT-treated lesions on the absolute value of Dx was evaluated using the Mann–Whitney *U*-test. Differences with *p*-values of <0.05 were considered statistically significant. Statistical calculations were performed with SPSS software, version 24.0 (SPSS Inc., Chicago, IL, USA).

Results

Dx% ranged from −3.4% to 6.8% (Table II). Dx was positive for all parameters for five (42%) patients and ranged from negative to positive for seven (58%) patients. The mean absolute values of Dx were 2.66 and 1.69 at D5 (p=0.755), 3.22 and 1.67 at D_{10} (p=0.048), 2.86 and 1.11 at D_{15} (p=0.018), 2.00 and 0.77 at D_{20} (p=0.048), 1.32 and 0.71 at D_{25} (p=0.106), 0.96 and 0.75 at D_{30} (p=0.343), and 0.74 and 0.72 at D35 (p=1.000) for ≥2 and <2 previous treatments, respectively, of lesions other than SBRT-treated lesions (Figure 1). Figures 2 and 3 show representative cases with large parametric discrepancies between DFH and DVH parameters.

Discussion

Because HCC patients often suffer from metachronous multicentric occurrence or intrahepatic metastasis and RT is not considered the first choice of treatment for HCC, most patients undergo other treatments, such as RFA and TACE, before RT (5, 13). A history of prior treatment may cause inhomogeneity in liver function (10). Our study revealed a discrepancy between DFH and DVH parameters and suggested that previous treatments influenced this parametric discrepancy.

The geometric relationship between the irradiated liver and previously treated lesions may influence the magnitude relationship between DFH and DVH parameters. Theoretically, when previous treatments are performed for lesions distant from SBRT-treated lesions and radioisotope (RI) non-accumulation occurs outside the irradiated liver parenchyma, the value of DFH parameters are greater than those of corresponding DVH parameters. In such cases, the risk of radiation-induced liver toxicity should be underestimated with DVH. By contrast, when previous treatments are performed for lesions close to SBRT-treated lesions and RI non-accumulation occurs within the irradiated liver parenchyma, the value of some DFH parameters is less

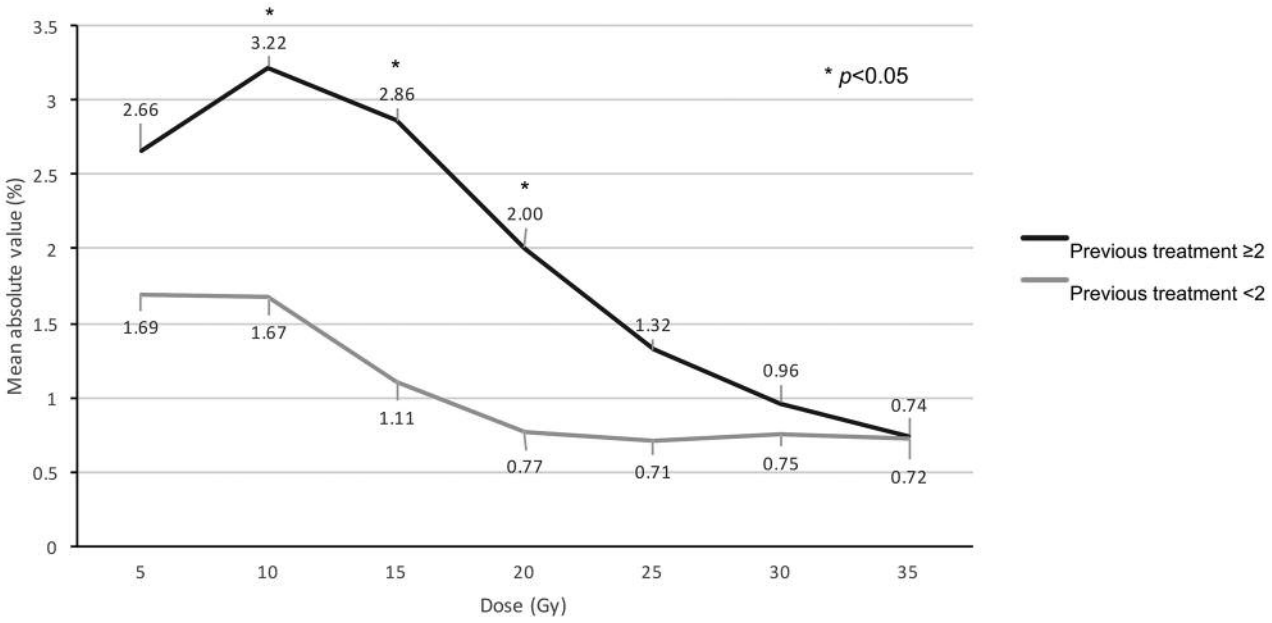

Figure 1. *Mean absolute values of the difference between Fx and Vx (Dx) according to the number of previous treatments of radiofrequency ablation, transarterial chemoembolization, and percutaneous ethanol injection therapy for lesions other than stereotactic body radiation therapy-treated lesions.*

than that of corresponding DVH parameters. In such cases, the risk of radiation-induced liver toxicity should be overestimated with DVH. In this study, the magnitude relationship between DFH and DVH parameters varied according to the doses, even for the same patients. In clinical settings, patients may receive multiple treatments for multiple sites of disease, and a lack of RI accumulation may be observed at various sites in the liver parenchyma. Hence, we could not identify a clear trend for the magnitude relationship between DFH and DVH parameters.

Dosimetric factors associated with toxicity are not well established for HCC patients treated with hypofractionated RT. Son *et al*. (14) treated 72 HCC patients using helical tomotherapy at 40–50 Gy in 10 fractions. They found that V_{15} was significantly associated with an increase in the Child–Pugh score. Liang *et al*. (15) treated 114 primary liver carcinomas using hypofractionated conformal RT at 40-68 Gy with a fraction size of 4-6 Gy. They found that V_{20} was an independent predictor of RILD. Dyk *et al*. (16) treated 23 patients with primary liver carcinomas using SBRT at 36-60 Gy in 3-6 fractions. They found that V_{25} was a predictor of decline in liver function after treatment. Although these reports evaluated patients with similar RT doses and fraction sizes, the recommended DVH parameters varied. The RT dose and fraction size of our patients were similar to those described in these previous reports, and the recommended parameters overlapped with the parameters of the significant discrepancy between DFH and DVH observed in our study. One possible reason for the variability in the recommended DVH parameters of the previous reports may be that the inhomogeneity of liver function was not considered. The use of DFH may facilitate the detection of dosimetric parameters for the precise prediction of radiation-induced liver toxicity.

Our study has certain limitations, including the relatively small number of patients who were examined. The previous treatments included RFA, TACE, and PEIT. We could not evaluate the differences in the influence of each treatment modality on the parametric discrepancy between DFH and DVH. We compared DFH and DVH parameters from a dosimetric perspective but could not compare the predictability of these parameters for radiation-induced liver toxicity. Further investigations are underway to address these issues.

In conclusion, previous treatments significantly influenced the parametric discrepancy between DFH and DVH. The use of DFH may facilitate the detection of dosimetric parameters for the precise prediction of radiation-induced liver toxicity.

Conflicts of Interest

None.

Acknowledgements

This work was supported by JSPS KAKENHI Grant Number 26861004.

The Authors wish to thank Ryuji Ikeda and Masato Maruyama, Kumamoto University Hospital, for their technical supports.

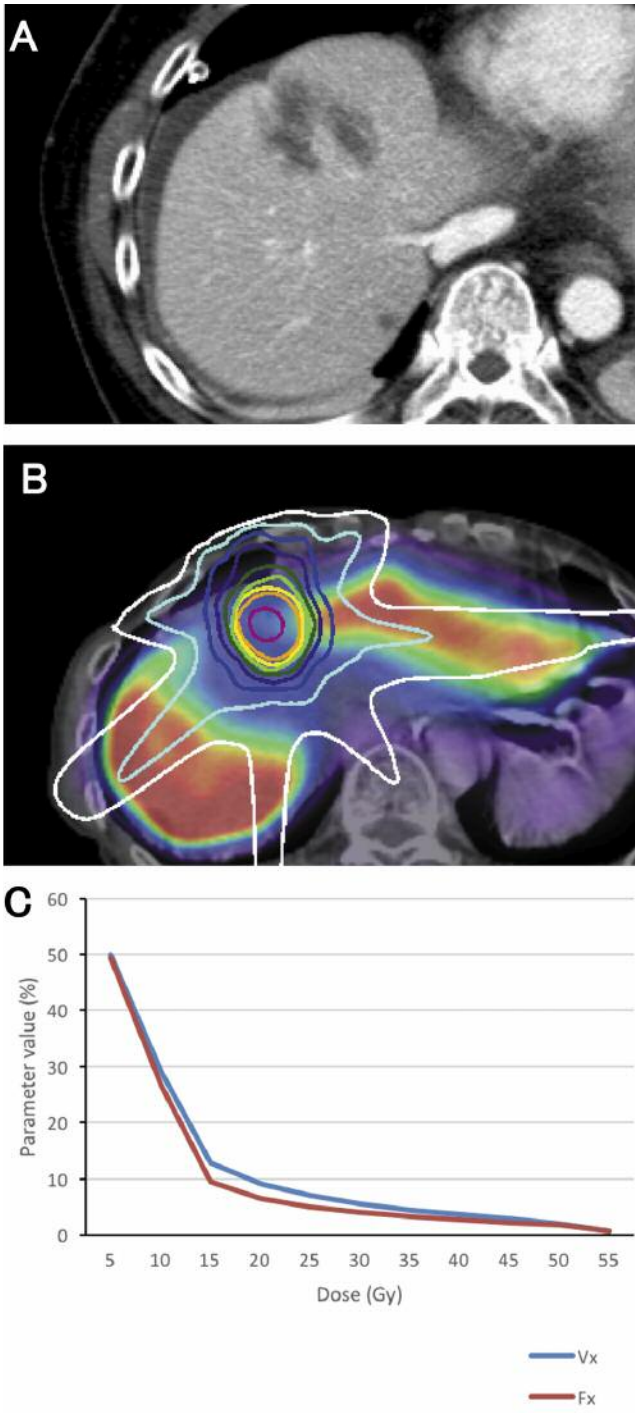

Figure 2. *A 63-year-old man with hepatocellular carcinoma (Patient 2). (A) Axial contrast-enhanced computed tomography (CT) image. He received radiofrequency ablation therapy twice for hepatocellular carcinoma in segment 8. (B) Fused image of single photon emission computed tomography (SPECT) and planning CT with the dose distribution of stereotactic body radiation therapy (SBRT). SPECT showed a decreased accumulation of the radioisotope around the treated area. We performed SBRT at 40 Gy for another lesion in segment 4. (C) The values of dose–function and dose–volume histogram parameters. F_{15} and V_{15} were 9.4% and 12.8%, respectively.*

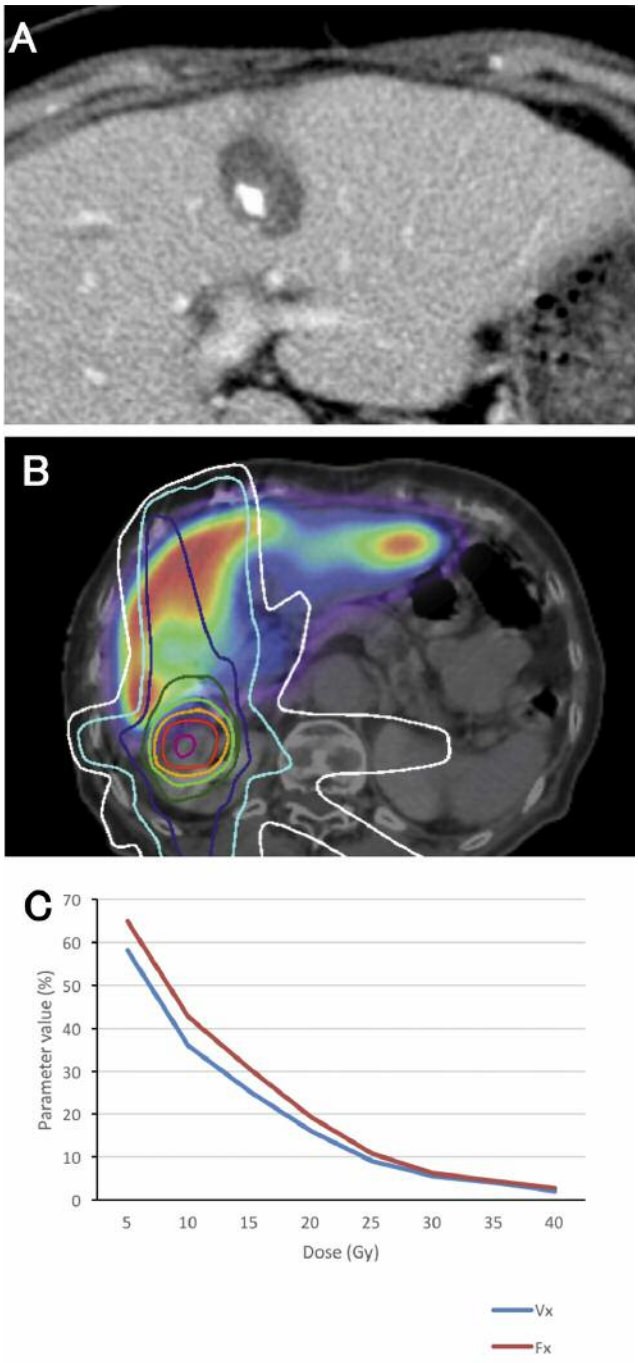

Figure 3. *A 79-year-old man with hepatocellular carcinoma (Patient 8). (A) Axial contrast-enhanced computed tomography (CT) image. He received transarterial chemoembolization and radiofrequency ablation for hepatocellular carcinoma in segment 3 and hepatic resection of segment 6. (B) Fused image of single photon emission computed tomography (SPECT) and planning CT with the dose distribution of stereotactic body radiation therapy (SBRT). SPECT showed a decreased accumulation of the radioisotope around the treated area in segment 3. We performed SBRT at 35 Gy for a recurrent lesion near the resected area of the remnant liver. (C) The values of dose–function and dose–volume histogram parameters. F_{10} and V_{10} were 42.7% and 36.0%, respectively.*

References

1 Klein J and Dawson LA: Hepatocellular carcinoma radiation therapy: review of evidence and future opportunities. Int J Radiat Oncol Biol Phys *87*: 22-32, 2013.

2 Seo YS, Kim MS, Yoo SY, Cho CK, Choi CW, Kim JH, Han CJ, Park SC, Lee BH, Kim YH and Lee DH: Preliminary result of stereotactic body radiotherapy as a local salvage treatment for inoperable hepatocellular carcinoma. J Surg Oncol *102*: 209-214, 2010.

3 Andolino DL, Johnson CS, Maluccio M, Kwo P, Tector AJ, Zook J, Johnstone PA and Cardenes HR: Stereotactic body radiotherapy for primary hepatocellular carcinoma. Int J Radiat Oncol Biol Phys *81*: e447-453, 2011.

4 Sanuki N, Takeda A, Oku Y, Mizuno T, Aoki Y, Eriguchi T, Iwabuchi S and Kunieda E: Stereotactic body radiotherapy for small hepatocellular carcinoma: a retrospective outcome analysis in 185 patients. Acta Oncol *53*: 399-404, 2014.

5 Toya R, Murakami R, Baba Y, Nishimura R, Morishita S, Ikeda O, Kawanaka K, Beppu T, Sugiyama S, Sakamoto T, Yamashita Y and Oya N: Conformal radiation therapy for portal vein tumor thrombosis of hepatocellular carcinoma. Radiother Oncol *84*: 266-271, 2007.

6 Pan CC, Kavanagh BD, Dawson LA, Li XA, Das SK, Miften M and Ten Haken RK: Radiation-associated liver injury. Int J Radiat Oncol Biol Phys *76*: S94-100, 2010.

7 Fukugawa Y, Namimoto T, Toya R, Saito T, Yuki H, Matsuyama T, Ikeda O, Yamashita Y and Oya N: Radiation-induced liver injury after 3D-conformal radiotherapy for hepatocellular carcinoma: quantitative assessment using Gd-EOB-DTPA-enhanced MRI. Acta Med Okayama *71*: 25-29, 2017.

8 Marks LB, Sherouse GW, Munley MT, Bentel GC and Spencer DP: Incorporation of functional status into dose-volume analysis. Med Phys *26*: 196-199, 1999.

9 Shirai S, Sato M, Suwa K, Kishi K, Shimono C, Kawai N, Tanihata H, Minamiguchi H and Nakai M: Single photon emission computed tomography-based three-dimensional conformal radiotherapy for hepatocellular carcinoma with portal vein tumor thrombus. Int J Radiat Oncol Biol Phys *73*: 824-831, 2009.

10 Tsuruga Y, Kamiyama T, Kamachi H, Shimada S, Wakayama K, Orimo T, Kakisaka T, Yokoo H and Taketomi A: Significance of functional hepatic resection rate calculated using 3D CT/(99m)Tc-galactosyl human serum albumin single-photon emission computed tomography fusion imaging. World J Gastroenterol *22*: 4373-4379, 2016.

11 Shimohigashi Y, Toya R, Saito T, Ikeda O, Maruyama M, Yonemura K, Nakaguchi Y, Kai Y, Yamashita Y, Oya N and Araki F: Tumor motion changes in stereotactic body radiotherapy for liver tumors: an evaluation based on four-dimensional cone-beam computed tomography and fiducial markers. Radiat Oncol *12*: 61, 2017.

12 Hanna GG, Van Sornsen De Koste JR, Carson KJ, O'Sullivan JM, Hounsell AR and Senan S: Conventional 3D staging PET/CT in CT simulation for lung cancer: impact of rigid and deformable target volume alignments for radiotherapy treatment planning. Br J Radiol *84*: 919-929, 2011.

13 Matsumoto Y, Fujii H, Matsuda M and Kono H: Multicentric occurrence of hepatocellular carcinoma: diagnosis and clinical significance. J Hepatobiliary Pancreat Surg *8*: 435-440, 2001.

14 Son SH, Kay CS, Song JH, Lee SW, Choi BO, Kang YN, Jang JW, Yoon SK and Jang HS: Dosimetric parameter predicting the deterioration of hepatic function after helical tomotherapy in patients with unresectable locally advanced hepatocellular carcinoma. Radiat Oncol *8*: 11, 2013.

15 Liang SX, Huang XB, Zhu XD, Zhang WD, Cai L, Huang HZ, Li YF, Chen L and Liu MZ: Dosimetric predictor identification for radiation-induced liver disease after hypofractionated conformal radiotherapy for primary liver carcinoma patients with Child-Pugh Grade A cirrhosis. Radiother Oncol *98*: 265-269, 2011.

16 Dyk P, Weiner A, Badiyan S, Myerson R, Parikh P and Olsen J: Effect of high-dose stereotactic body radiation therapy on liver function in the treatment of primary and metastatic liver malignancies using the Child-Pugh score classification system. Pract Radiat Oncol *5*: 176-182, 2015.

Received December 26, 2017
Revised January 22, 2018
Accepted January 24, 2018